

# Canonical Distribution Functions in Polymer Dynamics: II. Liquid–Crystalline Polymers

Patrick Ilg,<sup>1,\*</sup> Iliya V. Karlin,<sup>2</sup> Martin Kröger,<sup>3</sup> and Hans Christian Öttinger<sup>2</sup>

<sup>1</sup>*Institut für Theoretische Physik, Technische Universität Berlin, Hardenbergstr. 36, D-10623 Berlin, Germany*

<sup>2</sup>*ETH Zürich, Department of Materials, Institute of Polymers, CH-8092 Zürich, Switzerland*

<sup>3</sup>*Institut für Theoretische Physik, Technische Universität Berlin, Hardenbergstr. 36, D-10623 Berlin, Germany,  
ETH Zürich, Department of Materials, Institute of Polymers, CH-8092 Zürich, Switzerland*

(Dated: January 10, 2022)

The quasi-equilibrium approximation is employed as a systematic tool for solving the problem of deriving constitutive equations from kinetic models of liquid-crystalline polymers. It is demonstrated how kinetic models of liquid-crystalline polymers can be approximated in a systematic way, how canonical distribution functions can be derived from the maximum entropy principle and how constitutive equations are derived therefrom. The numerical implementation of the constitutive equations based on the intrinsic dual structure of the quasi-equilibrium manifold thus derived is developed and illustrated for particular examples. Finally, a measure of the accuracy of the quasi-equilibrium approximation is proposed that can be implemented into the numerical integration of the constitutive equation.

PACS numbers: 83.80.Xz, 83.10.Gr, 05.20.Dd, 05.10.-a

## I. INTRODUCTION

This paper continues a systematic approach to the derivation and numerical implementation of constitutive equations for complex fluids, initiated in Ref. [1]. In this approach, the systematic application of the quasi-equilibrium approximation to kinetic models is proposed, including the derivation of canonical distribution functions (CDF) and their use to obtain closed form constitutive equations. Also the natural numerical implementation of the resulting constitutive equations based on the dual structure of the quasi-equilibria is discussed together with a measure of the accuracy of the quasi-equilibrium approximation. While in Ref. [1] dilute solutions of flexible polymers were considered, the present paper extends this study to kinetic models of liquid-crystalline polymers. Peculiarities due to the mean-field nature of models for liquid crystalline polymers are discussed. A more detailed presentation of the subject can be found in [2].

Liquid-crystalline polymers have attracted considerable attention due to their capability of forming a highly oriented phase [3]. In polymer processing, for example, it is very important to understand the interplay between the tendency towards orientational ordering and the orientational effects due to the flow field [4, 5]. Kinetic models of liquid-crystalline (rigid rodlike) polymers were introduced by Hess and Doi [6, 7, 8] and are now used by many authors. Kinetic models of the dynamics of liquid-crystalline polymers are able to reproduce qualitatively most of the experimental results for the steady state in homogeneous flows [9]. Predictions of the kinetic models for transient viscoelastic phenomena are in general less reliable [10]. The main limitation of the kinetic model responsible for this failure is probably the neglect of defects of the orientational ordering. Recently, some work has been done in order to implement spatial variations of the orientational order into the kinetic model [11, 12]. For clarity, we restrict ourselves here to spatially homogeneous systems, and the corresponding kinetic models. The present approach can be easily extended to include also spatially inhomogeneous systems.

Numerical implementation of kinetic models of liquid-crystalline polymers in direct numerical flow calculations is in general very computationally intensive. However, kinetic models of polymer dynamics may serve as a starting point for the derivation of constitutive equations. In general, this derivation is not straightforward but requires approximations to the underlying kinetic model. The need for so-called closure approximations occurs in many branches of statistical physics and several suggestions for such approximations have been proposed in the literature (see e.g. [13] and references therein). A particularly successful approach for the derivation of constitutive equation is the so-called method of invariant manifold [14]. This method identifies relevant manifolds for the reduced description from which the constitutive equations can be derived. For example, it was found in Ref. [15] with the help of this method that the universal limit in the dynamics of dilute polymer solutions is given by the (revised) Oldroyd 8-constant model.

In Ref. [1] and in the present work, the quasi-equilibrium approximation is employed in order to derive a manifold formed by a set of canonical distribution functions (CDF). The quasi-equilibrium approximation is used successfully also in other branches of statistical physics, like for example chemical reaction kinetics, plasma and ferrofluids (see also Refs. [13, 16]). This approximation to the dynamics shows several desirable features like conservation of the dissipative nature of the dynamics, conservation

---

\*ilg@physik.tu-berlin.de

of positive-definiteness of distribution functions and a thermodynamic structure including dual variables. Improvements on this approximation can be found by either including more variables into the QEA, by constructing improved manifolds according to the method of invariant manifold proposed in Ref. [14] or by using a combined micro-macro simulation technique proposed in Ref. [17]. Here, we show how the quasi-equilibrium approximation can be used in order to obtain closed constitutive equations for liquid-crystalline polymers. We also present an algorithm for the numerical implementation of the constitutive equations. In addition, a measure for the accuracy of the approximation is suggested that does not require solutions to the kinetic model and can therefore be used while solving the constitutive equation.

Recently, the idea of using a set of canonical distribution functions (CDF), which are postulated and not based on the quasi-equilibrium approximation, for obtaining closures to kinetic models of dilute solutions of flexible polymers has also been used in Refs. [18, 19].

This paper is organized as follows. Kinetic models of the dynamics of liquid-crystalline polymers (LCPs) are reviewed in Sec. II. Canonical distribution functions and their use in the description of the dynamics of LCPs is described in Sec. III. Closed form constitutive equations are derived using CDF. Special emphasize is paid to so-called alignment tensor models. In Sec. V, a measure for the accuracy of the approximate description of polymer dynamics with CDF is proposed. In Sec. VI, some numerical results in steady shear flow are presented. Finally, some conclusions are offered in Sec. VII.

## II. KINETIC MODELS OF LIQUID-CRYSTALLINE POLYMERS

Consider a solution of liquid-crystalline polymers composed of rigid rodlike polymeric molecules. The kinetic models describe the microstate of liquid-crystalline polymers by the one-particle distribution function  $\psi(\mathbf{u}; t)$ , the probability density of finding a particle oriented along the unit vector  $\mathbf{u}$  at time  $t$ . For simplicity, only spatially homogeneous systems are considered.

### A. Kinetic Equations of Polymer Dynamics

Equations of motions for rigid rod models were proposed by Hess and Doi, [6, 7, 8], and can be found in most of the textbooks on polymer kinetic theory (see e.g. [3, 5, 9]). In the presence of a given homogeneous velocity gradient  $\boldsymbol{\kappa}$ , the time evolution of  $\psi$  may be written as

$$\partial_t \psi = -\hat{R}_{\mathbf{u}} \cdot [\mathbf{u} \times (\boldsymbol{\kappa} \cdot \mathbf{u} \psi)] + \hat{R}_{\mathbf{u}} \cdot \hat{D}_r \psi \hat{R}_{\mathbf{u}} \left( \frac{\delta F}{\delta \psi(\mathbf{u})} \right). \quad (1)$$

Here,  $\hat{R}_{\mathbf{u}} = \mathbf{u} \times \partial/\partial \mathbf{u}$  is the rotational operator,  $\partial/\partial \mathbf{u}$  the gradient on the unit sphere,  $\hat{D}_r$  the rotational diffusivity and  $\delta/\delta \psi$  the Volterra functional derivative. The dimensionless free energy functional per molecule,  $F[\psi] = F_0[\psi] + F_1[\psi]$ , can be split into the entropy of molecular alignment,

$$F_0[\psi] = \int d\mathbf{u} \psi(\mathbf{u}) \ln \psi(\mathbf{u}), \quad (2)$$

and the free energy contributions of interactions  $F_1$ . In the second virial approximation,  $F_1$  is given by

$$F_1[\psi] = \frac{\nu}{2} \langle\langle \beta(\mathbf{u}, \mathbf{u}') \rangle\rangle, \quad (3)$$

where  $\nu = n_p d \ell^2$  denotes the reduced excluded volume of  $n_p$  rods of length  $\ell$  and diameter  $d$  per unit volume. Here and below we use the following notations for averages:  $\langle f(\mathbf{u}) \rangle \equiv \int d\mathbf{u} f(\mathbf{u}) \psi(\mathbf{u})$ ,  $\langle\langle f(\mathbf{u}, \mathbf{u}') \rangle\rangle \equiv \iint d\mathbf{u} d\mathbf{u}' f(\mathbf{u}, \mathbf{u}') \psi(\mathbf{u}) \psi(\mathbf{u}')$ , where integration is performed over the three-dimensional unit sphere.

The kinetic equation (1) is supplemented by the expression for the polymer contribution to the stress tensor [9, 20],

$$\boldsymbol{\tau}^p[\psi] = -3n_p k_B T \left\langle [\mathbf{u} \times \hat{R}_{\mathbf{u}} \frac{\delta F}{\delta \psi(\mathbf{u})}] \mathbf{u} \right\rangle. \quad (4)$$

In Eq. (4), viscous contributions to  $\boldsymbol{\tau}^p$  are neglected since they are generally assumed to be negligible in liquid-crystalline polymers [9]. When Eq. (4) is used in the Navier-Stokes equations, the latter, together with the kinetic equation (1), constitute a closed system describing the dynamics of the solution.

The configuration dependent diffusion coefficient  $\hat{D}_r$  describes the hindrance of rotations due to neighboring rods. Following Doi and Edwards [9],  $\hat{D}_r$  is approximated by

$$\hat{D}_r \approx \overline{D}_r = D_r \left[ \frac{4}{\pi} \left\langle \left\langle \sqrt{1 - (\mathbf{u} \cdot \mathbf{u}')^2} \right\rangle \right\rangle \right]^{-2}, \quad (5)$$

where  $D_r$ , the rotational diffusion coefficient of a rod in an isotropic, semi-dilute solution of identical rods, is related to the rotational diffusion constant for a dilute solution,  $D_{r0}$ , by  $D_r = cD_{r0}(n_p\ell)^{-2}$  with an empirical coefficient  $c$ . It is generally believed that the self-consistent averaging approximation (5) does not alter the dynamics (1) qualitatively [21].

The nonlinearity of the kinetic equation (1) in  $\psi$  reflects the mean-field character of the model that provides an effective one-body description of the many-rod system. The equilibrium distribution,  $\psi^{\text{eq}}$ , corresponding to the stationary solution to the kinetic equation (1) in the absence of flow,  $\kappa = \mathbf{0}$ , is given by  $\psi^{\text{eq}} \propto \exp[-U]$ . The dimensionless self-consistent potential  $U$  is identified with

$$U(\mathbf{u}; \psi) = \frac{\delta F_1[\psi]}{\delta \psi(\mathbf{u})} = \nu \int d\mathbf{u}' \beta(\mathbf{u}, \mathbf{u}') \psi(\mathbf{u}'), \quad (6)$$

where Eq. (3) has been used.

If only excluded-volume interactions are considered, the dimensionless second virial coefficient  $\beta(\mathbf{u}, \mathbf{u}')$  for rigid rods was obtained by Onsager [22],

$$\beta(\mathbf{u}, \mathbf{u}') = |\mathbf{u} \times \mathbf{u}'| = \sqrt{1 - (\mathbf{u} \cdot \mathbf{u}')^2}. \quad (7)$$

Eq. (7) has a simple geometric interpretation since  $|\mathbf{u} \times \mathbf{u}'|$  is the area spanned by the vectors  $\mathbf{u}$  and  $\mathbf{u}'$ . The excluded-volume of two cylinders with length  $\ell$ , diameter  $d$  and orientations  $\mathbf{u}$  and  $\mathbf{u}'$  is therefore given by  $d\ell^2|\mathbf{u} \times \mathbf{u}'|$ . Thus,  $F_1$  decreases as the polymers orient in the same direction and finally leads to the nematic phase when the effect of the excluded-volume becomes sufficiently strong. Note, that the second virial approximation becomes exact in the limit of high aspect ratio,  $\ell/d \rightarrow \infty$ .

A variety of further expressions for  $F_1$  have been suggested in the literature [3]. A particular simple, phenomenological expression was given by Maier and Saupe [23, 24],

$$\beta^{\text{MS}}(\mathbf{u}, \mathbf{u}') = c_0 - c_1[(\mathbf{u} \cdot \mathbf{u}')^2 - \frac{1}{3}], \quad (8)$$

which together with Eq. (3) leads to

$$F_1^{\text{MS}}(\overline{\mathbf{a}_2}) = \frac{\nu}{2}[c_0 - c_1 \overline{\mathbf{a}_2} : \overline{\mathbf{a}_2}], \quad (9)$$

where  $c_0$  and  $c_1$  are parameters independent of  $\psi$ . In Eq. (9), the important notion of the orientational order parameter  $\overline{\mathbf{a}_2}$  is introduced,  $\overline{\mathbf{a}_2} = \langle \mathbf{u}\mathbf{u} - \frac{1}{3}\mathbf{1} \rangle$ . The isotropic state is characterized by  $\overline{\mathbf{a}_2} = \mathbf{0}$ , while  $\overline{\mathbf{a}_2} \neq \mathbf{0}$  indicates (nematic) orientational ordering.

The self-consistent equilibrium distribution corresponding to the potential (6) determines the isotropic nematic transition in equilibrium. The detailed form of the interaction potential can have significant effect on the behavior of the order parameter in the nematic phase. Specifically, the amount of order at the transition is known to be much smaller in the Maier-Saupe theory than in the Onsager model [25].

In the sequel, we consider generic interaction functionals of the form

$$F_1[\psi] = \bar{F}_1(\underline{M}), \quad (10)$$

where  $\underline{M} = \{M_1, \dots, M_{m_n}\} = \{\overline{\mathbf{a}_2}, \dots, \overline{\mathbf{a}_{2n}}\}$  denotes the set of irreducible (anisotropic) moments of the distribution function up to order  $2n$ ,  $(\overline{\mathbf{a}_{2n}})_{\alpha_1\beta_1\dots\alpha_n\beta_n} = \langle \overline{u_{\alpha_1}u_{\beta_1}\dots u_{\alpha_n}u_{\beta_n}} \rangle$ , and  $\overline{\mathbf{B}}$  denotes the symmetric irreducible part of the tensor  $\mathbf{B}$  [26]. In other words, the functional dependence of the interaction functional on the orientational distribution function  $\psi$  comes only through the dependence of the moments of  $\psi$ . For example, the tensor  $\overline{\mathbf{a}_2}$  contains five independent components. For convenience, these components are denoted by the scalars  $M_1, \dots, M_5$ . The total number of components of irreducible moments up to order  $2n$  is  $m_n$ . In case  $n = 1$  one has  $m_n = 5$ . In case  $n > 1$ , the components  $M_i$  for  $i > 5$  contain the independent components of the tensors  $\overline{\mathbf{a}_{2k}}$ ,  $k = 2, \dots, n$ .

The interaction functionals (10) correspond to virial coefficients of the form  $\beta(\mathbf{u}, \mathbf{u}') = \beta((\mathbf{u} \cdot \mathbf{u}')^2 - \frac{1}{3})$  with polynomials  $\beta(x)$  of degree  $n$ . The Maier-Saupe expression (9) is of the form (10) with  $n = 1$ . The Onsager potential (7), on the contrary, can only be cast into the form (10) for  $n \rightarrow \infty$ . In this case, systematic approximations of the form (10) with finite  $n$  have been proposed in [20]. The lowest order approximation to the free energy functional (3) obtained in [20] for the Onsager potential is

$$\bar{F}_1(\overline{\mathbf{a}_2}) = \frac{\nu}{\sqrt{6}} \sqrt{1 - \frac{3}{2} \overline{\mathbf{a}_2} : \overline{\mathbf{a}_2}}. \quad (11)$$

Some evidence was provided in [20] that the lowest order approximation represents a good approximation to  $F_1$  in case of the Onsager potential (7), at least on a representative subset of distribution functions.

Since the rotational diffusivity (5) is related to the Onsager interaction functional  $F_1$ , the same approximation can be employed to give [20]

$$\overline{D}_r = \overline{D}_r^{(n)}(\underline{M}). \quad (12)$$

Inserting the lowest order approximation for  $\bar{F}_1$  one obtains [20]

$$\overline{D}_r^{(1)} = (3\pi^2/32)D_r[1 - (3/2)\overline{\mathbf{a}}_2 : \overline{\mathbf{a}}_2]^{-1}. \quad (13)$$

The diffusion coefficient  $\overline{D}_r^{(1)}$  is positive in the entire physically meaningful range of the order parameter  $\overline{\mathbf{a}}_2$ . Expression (13) should be compared with the Doi phenomenological result

$$\overline{D}_{rD} = D_r[1 - (3/2)\overline{\mathbf{a}}_2 : \overline{\mathbf{a}}_2]^{-2}. \quad (14)$$

For highly oriented nematics the expression (13) is preferred compared to Doi's result [27]. It should be stressed that our derivation of the diffusion coefficient does not need any further assumptions or adjustable parameters, while the derivation of Eq. (14) requires the matching of  $\overline{D}_r$ , resp.  $F^{\text{int,MS}}$  in both, the isotropic and the fully ordered state [8, 9]. Since the rotational diffusivity  $\overline{D}_r$  is only determined within a phenomenological constant, the numerical factor  $3\pi^2/32$  in Eq. (13) can safely be put equal to one.

### B. H-Theorem

The time evolution of the free energy functional  $F = F_0 + F_1$  is given by

$$\dot{F} = \int d\mathbf{u} \frac{\delta F[\psi]}{\delta \psi(\mathbf{u})} \partial_t \psi(\mathbf{u}). \quad (15)$$

Inserting the kinetic equation (1) into Eq. (15) one obtains

$$\dot{F} = \kappa : \tau^p - \left\langle \hat{R}_{\mathbf{u}} \frac{\delta F[\psi]}{\delta \psi(\mathbf{u})} \cdot \bar{D}_r \hat{R}_{\mathbf{u}} \frac{\delta F[\psi]}{\delta \psi(\mathbf{u})} \right\rangle. \quad (16)$$

In the absence of a velocity gradient, the dynamics (1) drives the system irreversibly to the unique equilibrium state  $\psi^{\text{eq}}$  with  $F$  being an  $H$ -function of the relaxation dynamics. In the presence of a velocity gradient, Eq. (16) also describes the free energy exchange between the polymer and the solvent subsystem. The expression (4) for the stress tensor can be rewritten in terms of partial rather than functional derivatives if the free energy  $F$  is of the form  $F = F_0 + \bar{F}_1$ , with  $\bar{F}_1$  given by Eq. (10) depends on  $\psi$  only through moments,

$$\tau^p = 3n_p k_B T \overline{\mathbf{a}}_2 + \sum_{k=1}^n \left\langle [\mathbf{u} \times \hat{R}_{\mathbf{u}}(\overline{u_{\alpha_1} u_{\beta_1} \cdots u_{\alpha_k} u_{\beta_k}})] \mathbf{u} \right\rangle \frac{\partial \bar{F}_1}{\partial (\overline{\mathbf{a}}_{2k})_{\alpha_1 \beta_1 \cdots \alpha_k \beta_k}}. \quad (17)$$

In the special case  $n = 1$ , Eq. (17) simplifies to

$$\tau^p = 3n_p k_B T \overline{\mathbf{a}}_2 - 2 \frac{\partial \bar{F}_1}{\partial \overline{\mathbf{a}}_2} \cdot \mathbf{a}_2 + 2 \frac{\partial \bar{F}_1}{\partial \overline{\mathbf{a}}_2} : \mathbf{a}_4. \quad (18)$$

For the Maier–Saupe potential, Eq. (9), Eq. (18) coincides with the standard expression for the stress tensor given in [9].

### III. CANONICAL DISTRIBUTION FUNCTIONS IN POLYMER DYNAMICS

Within the kinetic models described in Sec. II, the dynamics and viscoelastic properties of liquid-crystalline polymers are given by Eqs. (1) and (4). In viscoelastic flow calculations, the combined simulation of the Navier–Stokes equations coupled with the kinetic equation (1) is computationally very intensive. Therefore, there has been considerable interest in deriving sufficiently accurate closed form constitutive equations from kinetic theory.

### A. The Closure Problem

Isotropic, uniaxially and biaxially oriented phases of LCPs are conveniently described by the order parameter tensor  $\overline{\mathbf{a}_2}$ . It is reasonable therefore to look for closed descriptions of the dynamics in terms of  $\overline{\mathbf{a}_2}$  alone. The description of the viscoelastic properties of LCPs in terms of the stress tensor (17), however, requires also the knowledge of moments up to order  $2n + 2$ . The time evolution of moments  $\overline{\mathbf{a}_{2j}}$  obtained from the kinetic equation (1) is of the form

$$\frac{d}{dt} \overline{\mathbf{a}_{2j}} = \mathbf{G}^{(2j)}(\overline{\mathbf{a}_2}, \dots, \overline{\mathbf{a}_{2j+2n}}) \quad (19)$$

with the functions

$$\begin{aligned} G_{\alpha_1 \beta_1 \dots \alpha_j \beta_j}^{(2j)}(\overline{\mathbf{a}_2}, \dots, \overline{\mathbf{a}_{2j+2n}}) &= \left\langle \hat{R}_{\mathbf{u}}[\overline{u_{\alpha_1} u_{\beta_1} \dots u_{\alpha_j} u_{\beta_j}}] \cdot (\mathbf{u} \times \boldsymbol{\kappa} \cdot \mathbf{u}) \right\rangle \\ &+ \bar{D}_r^{(n)} \left\langle \hat{R}_{\mathbf{u}}^2[\overline{u_{\alpha_1} u_{\beta_1} \dots u_{\alpha_j} u_{\beta_j}}] \right\rangle \\ &+ \bar{D}_r^{(n)} \sum_{k=1}^n \left\langle \hat{R}_{\mathbf{u}}[\overline{u_{\alpha_1} u_{\beta_1} \dots u_{\alpha_j} u_{\beta_j}}] \cdot \hat{R}_{\mathbf{u}}[\overline{u_{\alpha_1} u_{\beta_1} \dots u_{\alpha_k} u_{\beta_k}}] \right\rangle \frac{\partial \bar{F}_1}{\partial (\overline{\mathbf{a}_{2k}})_{\alpha_1 \beta_1 \dots \alpha_k \beta_k}}. \end{aligned} \quad (20)$$

Eqs. (19) and (20) form a hierarchy of moment equations where moments of order  $2j$  couple to moments of order  $(2j + 2n)$ . Therefore, closed form constitutive equations in terms of low order moments cannot be derived exactly from the kinetic equation but require some approximations of the distribution function. There exist an enormous amount of closure approximations as well as many numerical tests of the approximations in various flow situations (see, e.g. [8, 28, 29, 30, 31, 32]).

### B. Extremum Principle and Canonical Distribution Functions

Following the approach described in [1], we here derive closed form constitutive equations for LCPs by applying the so-called quasi-equilibrium approximation. Within this approximation, canonical distribution functions are obtained from the extremum principle under constraints [13, 16]

$$F[\psi] \rightarrow \min, \quad 1 = \int d\mathbf{u} \psi(\mathbf{u}), \quad M_k = \int d\mathbf{u} m_k(\mathbf{u}) \psi(\mathbf{u}) \quad (21)$$

for  $k = 1, \dots, m_n$ . Notice, that this principle does not coincide with the entropy maximum principle, because the free energy  $F$ , in general, is not proportional to the entropy. We consider in the sequel the special choice  $\overline{u_{\alpha_1} u_{\beta_1} \dots u_{\alpha_k} u_{\beta_k}}$  for the functions  $m_k(\mathbf{u})$ , such that  $\underline{M}$  represents the set of the first  $n$  irreducible moments of the distribution function already introduced in Eq. (10). Inserting the functional form  $F = F_0 + \bar{F}_1$ , where  $F_0$  is given by Eq. (2) and  $\bar{F}_1$  by Eq. (10), the solution to Eq. (21) is given explicitly as

$$\psi^*(\mathbf{u}) = \psi^{\text{eq}}(\mathbf{u}) \exp\left[\sum_{k=1}^{m_n} \Lambda_k m_k(\mathbf{u}) + \Lambda_0\right]. \quad (22)$$

The set of Lagrange multipliers  $\underline{\Lambda} = \{\Lambda_1, \dots, \Lambda_{m_n}\} = \{\overline{\Lambda_2}, \dots, \overline{\Lambda_{2n}}\}$  ensure the constraints in Eq. (21),

$$M_k = \int d\mathbf{u} m_k(\mathbf{u}) \psi^{\text{eq}}(\mathbf{u}) \exp\left[\sum_{j=1}^{m_n} \Lambda_j m_j(\mathbf{u}) + \Lambda_0\right], \quad (23)$$

and  $\Lambda_0$  ensures the normalization of  $\psi^*$ . The interpretation of the CDF (22) as a quasi-equilibrium distributions has already been given in [33].

The quasi-equilibrium free energy  $F^*$  is defined as  $F^* = F[\psi^*]$ . Inserting the form (22) one obtains

$$F^*(\underline{M}) = \sum_{k=1}^{m_n} \Lambda_k M_k + \Lambda_0. \quad (24)$$

Note, that although the interaction part of the free energy is given by Eq. (10), the total quasi-equilibrium free energy  $F^*$  cannot be expressed as a function of  $\underline{M}$  explicitly. This difficulty results from the fact that the normalization  $\Lambda_0$  of the distribution (22) cannot be evaluated analytically in general. From Eq. (24), the Lagrange multipliers can be interpreted as the conjugate to the macroscopic variables,

$$\Lambda_k = \frac{\partial F^*(\underline{M})}{\partial M_k}, \quad k = 1, \dots, m_n. \quad (25)$$

### C. Macroscopic dynamics

In the following, the canonical distribution functions (22) are employed in order to derive the macroscopic description of the polymer dynamics. We assume, that the CDF can be considered as representative states in the sense that a set of moments of the distribution function is approximated accurately by the corresponding moments evaluated with the CDF. A measure of the accuracy of this approximation is presented in Sec. V. For improvements on this approximation see [14, 17].

The macroscopic time evolution is defined as the time evolution of the macroscopic variables evaluated with the CDF,  $\dot{M}_k = \int d\mathbf{u} m_k(\mathbf{u}) \partial_t \psi^*$ . Inserting the kinetic equation (1) for  $\partial_t \psi$ , one finds

$$\dot{M}_k = \bar{G}_k(\underline{M}) \quad (26)$$

with

$$\bar{G}_k(\underline{M}) = \left\langle [\hat{R}_{\mathbf{u}} m_k(\mathbf{u})] \cdot (\mathbf{u} \times \boldsymbol{\kappa} \cdot \mathbf{u}) \right\rangle_{\Lambda} + \sum_{j=1}^{m_n} M_{kj}^* \Lambda_j, \quad (27)$$

where the symmetric, positive semi-definite matrix  $\mathbf{M}$  is defined by

$$M_{kj}^* = \bar{D}_{\Gamma}^{(n)} \left\langle [\hat{R}_{\mathbf{u}} m_k(\mathbf{u})] \cdot [\hat{R}_{\mathbf{u}} m_j(\mathbf{u})] \right\rangle_{\Lambda} \quad (28)$$

Eqs. (26), (27), (28) together with Eq. (22) represent the closed set of macroscopic equations. The constitutive relation is obtained by evaluating the stress tensor (4) with the CDF,  $\boldsymbol{\tau}^{p,*}(\underline{M}) = \boldsymbol{\tau}^p[\psi^*]$ . Here, it reads

$$\boldsymbol{\tau}^{p,*}(\underline{M}) = -3n_p k_B T \sum_{k=1}^{m_n} \left\langle [\mathbf{u} \times \hat{R}_{\mathbf{u}} m_k(\mathbf{u})] \mathbf{u} \right\rangle_{\Lambda} \frac{\partial F^*(\underline{M})}{\partial M_k} \quad (29)$$

The macroscopic free energy change,  $\dot{F}^*$ , is found from Eqs. (16) and (26) to be given by

$$\dot{F}^* = \boldsymbol{\kappa} : \boldsymbol{\tau}^{p,*} - \sum_{k,j=1}^{m_n} \Lambda_k M_{kj}^* \Lambda_j \quad (30)$$

and could have been obtained also by evaluating the free energy change (16) on the CDF (22). In the absence of flow, the free energy change (30) is negative semi-definite as is the underlying kinetic model.

### D. Alignment Tensor Models

So far, the macroscopic description of LCP considered in the literature has almost exclusively considered the order parameter tensor  $\overline{\mathbf{a}_2}$  as the only macroscopic variables. In our notation, this corresponds to the special choice of the order parameter tensor  $\overline{\mathbf{a}_2}$  as the only macroscopic variable,  $n = 1$  and  $\overline{\mathbf{a}_2} = \langle \overline{\mathbf{u}\mathbf{u}} \rangle$ . Due to symmetry,  $\overline{\mathbf{a}_2}$  is the lowest non-trivial moment of  $\psi$ .

In this approximation, the dimensionless mean-field interaction potential derived from the free energy functional in case of the Onsager potential reads [20],

$$U^{(1)}(\mathbf{u}, \overline{\mathbf{a}_2}) = \frac{\nu}{\sqrt{6}} \frac{1 - \frac{3}{2} \mathbf{u}\mathbf{u} : \overline{\mathbf{a}_2}}{\sqrt{1 - \frac{3}{2} \overline{\mathbf{a}_2} : \overline{\mathbf{a}_2}}}, \quad (31)$$

which can be compared to the expression for the Maier-Saupe potential

$$U_{\text{MS}}(\mathbf{u}, \overline{\mathbf{a}_2}) = c_2 - c_1 \nu \mathbf{u}\mathbf{u} : \overline{\mathbf{a}_2}, \quad (32)$$

where  $c_2$  is an arbitrary constant.

In this approximation, the canonical distribution function (22) reduces to

$$\psi_{\Lambda}^*(\mathbf{u}) = \exp[-\nu \beta'(\overline{\mathbf{a}_2} : \overline{\mathbf{a}_2}) \overline{\mathbf{a}_2} + \overline{\boldsymbol{\Lambda}_2}) : \mathbf{u}\mathbf{u} + \Lambda_0] / Z^{(1)}. \quad (33)$$

The Lagrange multipliers  $\overline{\boldsymbol{\Lambda}_2}$  form a symmetric traceless matrix dual to  $\overline{\mathbf{a}_2}$ . The quasi-equilibrium distribution (33) not only reduces to the equilibrium distribution for  $\overline{\boldsymbol{\Lambda}_2} = \mathbf{0}$  but also gives the exact steady state solution  $\overline{\boldsymbol{\Lambda}_2}^{\text{ss}} = -\dot{\gamma}/2$  for

homogeneous potential flows. Due to the occurrence of the second moment  $\overline{\mathbf{a}_2}$ , the quasi-equilibrium states  $\psi_\Lambda^*$  have to be determined self-consistently. Further manipulations are simplified by introducing new variables  $\Theta = \overline{\Lambda_2} - \nu\beta'(\overline{\mathbf{a}_2} : \overline{\mathbf{a}_2})\overline{\mathbf{a}_2}$  and  $\Theta_0 = \Lambda_0 - \ln Z^{(1)}$ , where  $\Theta$  is a symmetric, traceless matrix. In terms of new variables, the quasi-equilibrium states (33) take the form

$$\psi^*(\mathbf{u}) = \exp[\mathbf{u} \cdot \Theta \cdot \mathbf{u} + \Theta_0], \quad (34)$$

where  $\Theta_0$  ensures the normalization of  $\psi^*$ . The distribution (34) is sometimes termed Bingham distribution.

Accordingly, the diffusion coefficient  $\overline{D}_r$  is approximated by  $\overline{D}_r^{(1)}$  given in Eq. (13). In the following, the macroscopic time evolution equations for  $\overline{\mathbf{a}_2}$  are obtained from Eqs. (26), (27), (28) and read,

$$\dot{\overline{\mathbf{a}_2}} = \mathbf{G}_h^*(\overline{\mathbf{a}_2}) + \mathbf{G}_d^*(\overline{\mathbf{a}_2}). \quad (35)$$

The presence of a flow field gives raise to the contribution  $\mathbf{G}_h^*$  in Eq. (35),

$$\mathbf{G}_h^*(\overline{\mathbf{a}_2}) = \boldsymbol{\kappa} \cdot \overline{\mathbf{a}_2} + \overline{\mathbf{a}_2} \cdot \boldsymbol{\kappa}^T + \frac{1}{3}\dot{\boldsymbol{\gamma}} - \dot{\boldsymbol{\gamma}} : \mathbf{a}_4^*, \quad (36)$$

where  $\dot{\boldsymbol{\gamma}} = \boldsymbol{\kappa} + \boldsymbol{\kappa}^T$  denotes the rate-of-strain tensor and  $\mathbf{a}_4^* = \langle \mathbf{u}\mathbf{u}\mathbf{u}\mathbf{u} \rangle_\Lambda$  is evaluated with the Bingham distribution (34). The contribution  $\mathbf{G}_d^*$  of the Brownian motion and the interaction potential is given by

$$\mathbf{G}_d^*(\overline{\mathbf{a}_2}) = \mathbf{M}^* : \overline{\Lambda_2}, \quad (37)$$

where  $\overline{\Lambda_2} = \partial F^*(\overline{\mathbf{a}_2}) / \partial \overline{\mathbf{a}_2}$  and the matrix  $\mathbf{M}^*$  is given by

$$M_{\alpha\beta\mu\nu}^* = \overline{D}_r(\delta_{\alpha\mu}(\overline{\mathbf{a}_2})_{\beta\nu} + \delta_{\alpha\nu}(\overline{\mathbf{a}_2})_{\beta\mu} + \delta_{\beta\mu}(\overline{\mathbf{a}_2})_{\alpha\nu} + \delta_{\beta\nu}(\overline{\mathbf{a}_2})_{\alpha\mu} - 4(\mathbf{a}_4^*)_{\alpha\beta\mu\nu}).$$

In Eq. (38), use has been made of the fact that the approximated diffusion coefficient  $\overline{D}_r$  is independent of the orientation  $\mathbf{u}$ . Inserting the expression for the free energy one arrives at

$$\mathbf{G}_d^*(\overline{\mathbf{a}_2}) = -6\overline{D}_r^{(1)}\overline{\mathbf{a}_2} + 6\overline{D}_r^{(1)}\nu\beta'(\overline{\mathbf{a}_2} : \overline{\mathbf{a}_2})(\overline{\mathbf{a}_2} \cdot \overline{\mathbf{a}_2} + \frac{1}{3}\overline{\mathbf{a}_2} - \overline{\mathbf{a}_2} : \mathbf{a}_4^*), \quad (38)$$

The Bingham distribution (34) has already been employed in the literature [30, 34] to derive closed form constitutive equations from the kinetic model (1). However, the expression for  $\mathbf{G}_d^*$  differs from the results given in [30, 34] not only in the diffusion coefficient  $\overline{D}_r^{(1)}$ . It also generalizes earlier result to general interaction potentials of the form (10). For the approximation (31) to the Onsager potential, for example, a non-polynomial dependence on the order parameter  $\overline{\mathbf{a}_2}$  occurs, which becomes important in the nematic state [20]. Comparative studies of various closure approximations to the kinetic model for the Maier-Saupe potential have clearly demonstrated that closures based on the Bingham distribution are preferable compared to more ad hoc closure approximations [28].

In the present case, the macroscopic free energy (24) reduces to

$$F^*(\overline{\mathbf{a}_2}) = \overline{\Lambda_2} : \overline{\mathbf{a}_2} + \Lambda_0. \quad (39)$$

The macroscopic polymer contribution to the stress tensor (29) simplifies to

$$\boldsymbol{\tau}^{P,*} = 2k_B T \left( \overline{\mathbf{a}_2} \cdot \overline{\Lambda_2} - \mathbf{a}_4^* : \overline{\Lambda_2} \right). \quad (40)$$

Expression (40) is also obtained when the macroscopic entropy (39) is inserted into Eq. (4).

#### IV. NUMERICAL INTEGRATION SCHEME

Eqs. (26) are the closed form macroscopic equations. Together with the expression (29) for the stress tensor they provide the macroscopic constitutive equation of the system. However, the time evolution equations (26) still contain the Lagrange multipliers, that have to be determined such that the constraints in Eq. (21) are satisfied.

To deal with this situation, a numerical integration scheme for the macroscopic equations in the context of dilute solutions of flexible polymers has been proposed in Ref. [1]. This scheme is general enough to be applied also to the present situation. We present here this integration scheme only briefly, referring the reader to [1] for further details.

### A. Dynamics of Dual Variables

In the extremum principle (21), the Lagrange multipliers occur naturally to satisfy the constraints. Due to Eq. (25), the Lagrange multipliers are interpreted as conjugate variables. Instead of eliminating the Lagrange multipliers  $\underline{\Lambda}$  in favor of the macroscopic variables  $\underline{\Lambda} = \underline{\Lambda}(\underline{M})$ , the Lagrange multipliers play the role as dynamical variables that determine the values of the macroscopic variables,  $\underline{M} = \underline{M}(\underline{\Lambda})$ . Note, that the functions  $\underline{M}(\underline{\Lambda})$  are given by Eq. (23). With the help of the Legendre transform of the macroscopic free energy,  $G(\underline{\Lambda}) = F^*(\underline{M}) + \sum_{k=1}^{m_n} \Lambda_k M_k$ , the time evolution of  $\underline{\Lambda}$  is given by

$$\dot{\Lambda}_k = \sum_{j=1}^{m_n} (\mathbf{C})_{kj}^{-1} \dot{M}_j(\underline{\Lambda}), \quad (41)$$

where  $\mathbf{C}^{-1}$  is the inverse of the matrix  $C_{kj} = \partial^2 G(\underline{\Lambda}) / \partial \Lambda_k \partial \Lambda_j$  and  $\dot{M}_j(\underline{\Lambda})$  is given by the right hand side of Eq. (26).

### B. Numerical Integration Scheme

The reformulation of the macroscopic dynamics (26) in terms of the dual variables  $\underline{\Lambda}$  described in Sec. IV A is suitable for numerical implementation. The Lagrange multipliers  $\underline{\Lambda}$  now play the role of independent dynamic variables, instead of  $\underline{M}$ . In order to advance given values  $\underline{\Lambda}(t)$  at time  $t$  to their values  $\underline{\Lambda}(t + \tau)$ , with small time step  $\tau$ , the following first order integration scheme is proposed in Ref. [1]:

1. The new values of the macroscopic variables  $\underline{M}(t + \tau)$  are found from the values  $\underline{\Lambda}(t)$  by

$$\frac{M_k(t + \tau) - M_k(t)}{\tau} = G_k(\underline{M}(\underline{\Lambda}(t))), \quad (42)$$

where  $G_k(\underline{M})$  denotes the right hand side of Eq. (26) with  $\underline{\Lambda}(t)$  the actual values of the Lagrange multipliers.

2. The matrix  $C_{kj}$  is evaluated from

$$C_{kj}(t) = \langle m_k m_j \rangle_{\Lambda}(t) - M_k(t) M_j(t), \quad (43)$$

where  $\langle m_k m_l \rangle_{\Lambda}$  is calculated with the distribution function (22) where  $\underline{\Lambda} = \underline{\Lambda}(t)$ .

3. The  $n \times n$  matrix  $\mathbf{C}(t)$  is inverted numerically to give  $\mathbf{C}^{-1}(t)$ .
4. The values of the Lagrange multipliers,  $\underline{\Lambda}(t + \tau)$ , are given by

$$\frac{\Lambda_k(t + \tau) - \Lambda_k(t)}{\tau} = \sum_{j=1}^{m_n} C_{kj}^{-1}(t) \frac{M_j(t + \tau) - M_j(t)}{\tau} \quad (44)$$

This concludes one time step of integration. The integration scheme has to be supplemented by initial conditions  $\underline{\Lambda}(0)$ . The special case of equilibrium initial conditions corresponds to  $\underline{\Lambda}(0) = \underline{0}$ . The appearance of the correlation matrix  $\mathbf{C}$  as a tool to recompute moments into Lagrange multipliers in this scheme is intimately related to the structure of the quasi-equilibrium approximation.

Note, that evaluating the matrix  $\mathbf{C}$  requires moments of  $\Psi$  which are of higher order than the macroscopic variables themselves. If  $n$  denotes the number of macroscopic variables, the numerical integration scheme requires in total  $n(n+3)/2$  integrals per time step to evaluate  $\underline{M}$  and  $\mathbf{C}$ . Due to the symmetry of  $\mathbf{C}$ , this number is of order  $n^2/2$  rather than  $n^2$ . The evaluation of all these integrals with standard numerical methods might be time-consuming, especially for high-dimensional integrals. It is demonstrated in [35] that under certain circumstances these integrals can be evaluated efficiently by adapting methods of fast Fourier transformations. This computational issue is out of scope of this paper.

### C. Numerical Implementation of Alignment Tensor Models

For the special case of alignment tensor models described in Sec. III D, the general integration scheme outlined in Sec. IV B is applied. The integrals over the unit sphere associated with the evaluation of moments of the canonical distribution function are performed numerically. Different resolutions of the numerical integration are used to obtain more accurate results by extrapolating to infinite resolution. The normalization of  $\mathbf{u}$ ,  $\mathbf{u}^2 = 1$ , and the consistency relations  $\langle \mathbf{u}\mathbf{u}\mathbf{u}\mathbf{u} \rangle_{\Lambda} : \mathbf{1} = \langle \mathbf{u}\mathbf{u} \rangle_{\Lambda}$  are



used as additional checks of the results of the numerical integration. The inversion of the matrix  $\mathbf{C}$  is done by using the explicit expression for the inverse of a symmetric  $6 \times 6$  matrix as given by the symbolic computation software Mathematica<sup>TM</sup>. The Lagrange multipliers are advanced by Eq. (44). The resulting algorithm has been implemented and tested under various circumstances. This numerical implementation differs from the one proposed in [30]. In the latter reference, approximate expressions for the eigenvalues of  $\mathbf{a}_4^*$  as a function of the eigenvalues of  $\overline{\mathbf{a}_2}$  are proposed, whereas in the present approach the necessity of expressing the Lagrange multipliers  $\underline{\Lambda}$  in terms of the moments is circumvented by the scheme (42)–(44). Together with suitable rotations to diagonalizing coordinate systems, these expressions allow direct numerical integration of Eq. (35).

## V. ACCURACY OF THE APPROXIMATION BY CDF

The use of the CDFs for the macroscopic description described in Sec. III C imposes approximations to the underlying dynamics. Therefore, the accuracy of this approximation needs to be discussed.

The accuracy of the approximation by CDFs can be studied in two ways: First, the result of integrating the macroscopic dynamics can be compared to direct numerical integration (e.g. by Brownian dynamics) of the underlying kinetic model. Alternatively, the dynamic variance  $\Delta$  that plays a central role in the method of invariant manifold [14] may be used in order to access the accuracy of the approximation. The advantage of using  $\Delta$  to estimate the accuracy of the approximation is that it can be evaluated while integrating the macroscopic dynamics, *without* performing numerics for the underlying microscopic dynamics. For the use of the dynamic variance in a mixed micro–macro computation see [17].

The dynamic variance  $\Delta$  is defined as

$$\Delta(\mathbf{u}; \underline{\mathbf{M}}) = J\psi^* - \sum_{j=1}^{m_n} \frac{\partial \psi^*}{\partial M_j} \dot{M}_j^*, \quad (45)$$

where  $J\psi^*$  denotes the right hand side of Eq. (1) evaluated with the CDF  $\psi^*$ ,

$$J\psi^* = -\hat{R}_{\mathbf{u}} \cdot [\mathbf{u} \times (\boldsymbol{\kappa} \cdot \mathbf{u}\psi^*)] + \overline{D}_r \sum_k^{m_n} \hat{R}_{\mathbf{u}} \cdot \psi^* \hat{R}_{\mathbf{u}} m_k(\mathbf{u}) \Lambda_k. \quad (46)$$

The dynamic variance  $\Delta$  can be interpreted as the difference of the microscopic time evolution evaluated with  $\psi^*$ , Eq. (46), and the time evolution of the CDFs due to the macroscopic dynamics. If  $\Delta \equiv 0$ , the CDFs are said to form an invariant manifold of the dynamics (1). In case  $\Delta \neq 0$ , the method of invariant manifold uses  $\Delta$  to obtain improved manifolds of distribution functions. Here and in a companion paper [1],  $|\Delta|$  is used as a measure of the accuracy of the approximation by CDFs, where the norm  $|\bullet|$  is specified later.

Consider functions  $Y_k(\underline{\mathbf{M}})$  defined by  $Y_k(\underline{\mathbf{M}}) \equiv \int d\mathbf{u} y_k(\mathbf{u}) \Delta(\mathbf{u}; \underline{\mathbf{M}})$ . Some choices of  $y_k(\mathbf{u})$  are discussed below. The functions  $Y_k$  can be interpreted as the difference of the time evolution of the macroscopic moments if evaluated from the microscopic dynamics and from the macroscopic dynamics. For the special case of alignment tensor models, introduced in Sec. III D, functions  $Y_k$  found from Eq. (45) read

$$Y_k = \left\langle y_k(\mathbf{u}) \mathbf{u} \mathbf{u} : [3\boldsymbol{\kappa} - 2\boldsymbol{\Theta} \cdot \mathbf{P} \cdot \boldsymbol{\kappa} + 4\overline{D}_r \boldsymbol{\Theta} \cdot \mathbf{P} \cdot \overline{\Lambda}_2 - 6\overline{D}_r \overline{\Lambda}_2] \right\rangle_{\Lambda} - [\langle y_k(\mathbf{u}) (\mathbf{u} \mathbf{u}) \rangle_{\Lambda} - \langle y_k(\mathbf{u}) \rangle_{\Lambda} \langle \mathbf{u} \mathbf{u} \rangle_{\Lambda}] : \frac{\partial \boldsymbol{\Theta}}{\partial \overline{\mathbf{a}_2}} : \dot{\overline{\mathbf{a}_2}}, \quad (47)$$

where  $\mathbf{P} = \mathbf{1} - \mathbf{u} \mathbf{u}$  is the projector perpendicular to  $\mathbf{u}$ ,  $\dot{\overline{\mathbf{a}_2}}$  is given by Eq. (35) and

$$\frac{\partial \boldsymbol{\Theta}}{\partial \overline{\mathbf{a}_2}} = \mathbf{C}^{-1} - \nu \beta' \mathbf{1} \mathbf{1} - 2\nu \beta'' \overline{\mathbf{a}_2} \overline{\mathbf{a}_2}. \quad (48)$$

We have  $Y_0 = 0$  for  $y_0 = 1$ , since the first and second term in Eq. (45) conserve the normalization of the distribution function independently. Further,  $Y_k$  vanishes by construction if  $y_k$  corresponds to components of the tensor  $\mathbf{u} \mathbf{u}$ . For  $y_k$  corresponding to  $\mathbf{u} \mathbf{u} \mathbf{u} \mathbf{u}$  or higher order tensors, the quantities  $Y_k$  contain valuable information about the variance  $\Delta$  and may be used as a measure for  $|\Delta|$ .

## VI. SOME NUMERICAL RESULTS

In the present section, the macroscopic equations (37) with (34) are integrated numerically using the dual integrator presented in Sec. IV B.

### A. Some Numerical Results for Steady Shear Flow

The integration scheme described above was used to obtain the time evolution of the macroscopic variables  $\overline{\mathbf{a}_2}$  from Eq. (37) in steady shear flow. The functions  $\mathbf{G}$  and  $\mathbf{F}$  are given in Eqs. (36) and (38), respectively with  $\kappa_{\alpha\beta} = \dot{\gamma}\delta_{\alpha 1}\delta_{\beta 2}$ . We employ the approximation (31) to the Onsager excluded volume potential and expression (13) for the diffusion coefficient. The minimal value  $\nu_2$  of the nematic potential that allows only a stable nematic phase was estimated from steady state values of the numerical solution of Eq. (37) in the absence of flow,  $\mathbf{G} = \mathbf{0}$ . For almost isotropic initial conditions a value  $\nu_2 \approx 6.5$  was obtained. Following Larson [36], we set  $\nu_2$  equal to this minimal value. Fig. 1 shows the dimensionless shear viscosity as a function of shear strain for two low values of the dimensionless shear rate  $\text{Pé}$  as obtained from the numerical integration for equilibrium initial condition. The Péclet number  $\text{Pé}$  is defined as the dimensionless shear rate  $\text{Pé} = \dot{\gamma}/6D_r^*$ , where  $D_r^*$  is the diffusion coefficient  $D_r$  defined in Eq. (5) and below at the concentration  $\nu_2$ . It is obvious from Fig. 1 that the present macroscopic description shows a so-called ‘tumbling’ or ‘wagging’ regime [36].

Rheological and rheo-optical experiments on lyotropic solutions of rodlike polymers have clearly demonstrated the existence of a ‘tumbling’ or ‘wagging’ regime for low shear rates. In Fig. 2, the experimental result for the shear viscosity of the lyotropic nematic polymer n-octylcyanobiphenyl is given as reported in [37]. Note, that the experimental results of Refs. [37, 38] are obtained from birefringence data of a monodomain liquid-crystalline polymer. Therefore, neglecting spatial inhomogeneities in the kinetic model is justified. The experimental data were obtained in a parallel-plate flow from birefringence measurements for a shear rate of  $\dot{\gamma} = 16\text{s}^{-1}$ . Qualitatively, the simulation results show similar behavior than the experimental findings. However, the damping of the oscillations of the shear viscosity is not seen in Fig. 1. The authors of Ref. [37] speculate that this behavior might be due to out-of-plane director orientations. Another dissipative mechanism not included in the present kinetic model is translational diffusion which could also explain the damping of the oscillations in Fig. 1. We mention, that the authors of Ref. [38] obtained a fit to experimental data on a similar liquid-crystalline polymer which is comparable to our simulation results. Their procedure requires fitting of three parameters of a generalized version of Ericksen’s theory of nematic liquid crystals [39].

## VII. CONCLUSION

A systematic approach to the derivation and implementation of constitutive equations proposed in [1] is applied in the present work to the dynamics of liquid-crystalline polymers. Employing the quasi-equilibrium approximation, a set of canonical distribution functions is obtained which is further used to derive constitutive equations. The numerical implementation and a measure of the accuracy of the approximation is discussed. The present approach is illustrated for the kinetic model of liquid-crystalline polymers with the Onsager excluded volume potential in steady shear and steady elongational flow.

### Acknowledgments

This research was supported in part by the National Science Foundation under grant No. PHY99-07949.

- 
- [1] P. Ilg, I. V. Karlin, H. C. Öttinger, Canonical Distribution Functions in Polymer Dynamics: I. Dilute Solutions of Flexible Polymers, preprint 2001.
  - [2] P. Ilg, Reduced Description of Kinetic Models of Polymer Dynamics, Wissenschaft & Technik Verlag, Berlin, 2001.
  - [3] P. G. de Gennes, The Physics of Liquid Crystals, Clarendon Press, Oxford, 1974.
  - [4] W. R. Burghardt, Molecular orientation and rheology in sheared lyotropic liquid crystalline polymers, *Macromol. Chem. Phys.* 199 (1998) 471-488.
  - [5] R. B. Bird, C. F. Curtiss, R. C. Armstrong, O. Hassager, Dynamics of Polymeric Liquids, Vol. 2, Kinetic Theory, Wiley, New York, 1987.
  - [6] S. Hess, Fokker-Planck-equation approach to flow alignment in liquid crystals, *Z. Naturforsch.* 31A (1976) 1034-1037.
  - [7] S. Hess, Pre- and post-translational behavior of the flow alignment and flow-induced phase transition in liquid crystals, *Z. Naturforsch.* 31A (1976) 1507-1513.
  - [8] M. Doi, Molecular dynamics and rheological properties of concentrated solutions of rodlike polymers in isotropic and liquid crystalline phases, *J. Polym. Sci., Polym. Phys. Ed.* 19 (1981) 229-243.
  - [9] M. Doi, S. F. Edwards, The Theory of Polymer Dynamics, Oxford University Press, Oxford, 1986.
  - [10] K. F. Wissbrun, Rheology of Rod-like Polymers in the Liquid Crystalline State, *J. Rheol.* 25 (1981) 619-662.
  - [11] M. Kröger, H. S. Sellers, A molecular theory for spatial inhomogeneous, concentrated solutions of rod-like liquid crystals, in *Lecture Notes in Physics, Complex Fluids*, Springer, New York, 1992, 295-301.

- [12] J. J. Feng, G. Sgaliari, L. G. Leal, A theory for flowing nematic polymers with orientational distortion *J. Rheol.* 44 (2000) 1085-1101. Erratum: *ibid.* 1435.
- [13] R. Balian, *From Microphysics to Macrophysics*. Vol. 2, Springer, Berlin, 2nd Ed., 1992.
- [14] A. N. Gorban, I. V. Karlin, Method of Invariant Manifolds and Regularization of Acoustic spectra, *Transp. Theor. Stat. Phys.* 23 (1994) 559-632.
- [15] V. B. Zmievski, I. V. Karlin, M. Deville, The universal limit in dynamics of dilute polymeric solutions, *Physica A* 275 (2000) 152-177.
- [16] A. N. Gorban, *Equilibrium Encircling*, Chapt. 3, Quasi-Equilibrium Entropy Maximum, pp. 99-122. Nauka, Novosibirsk, 1984.
- [17] A. N. Gorban, I. V. Karlin, P. Ilg, H. C. Öttinger, Corrections and Enhancements of Quasi-Equilibrium States, *J. Non-Newton. Fluid Mech.* 96 (2001) 203-219.
- [18] G. Lielens, P. Halin, I. Jaumin, R. Keunings, V. Legat, New Closure Approximations for the Kinetic Theory of Finitely Extensible Dumbbells, *J. Non-Newton. Fluid Mech.* 76 (1998) 249-279.
- [19] G. Lielens, R. Keunings, V. Legat, The FENE-L and FENE-LS Closure Approximation to the Kinetic Theory of Finitely Extensible Dumbbells, *J. Non-Newton. Fluid Mech.* 87 (1999) 279-296.
- [20] P. Ilg, I. V. Karlin, H. C. Öttinger, Generating moment equations in the Doi model of liquid-crystalline polymers, *Phys. Rev. E* 60 (1999) 5783-5787.
- [21] R. G. Larson, H. C. Öttinger, Effect of molecular elasticity on the out-of-plane orientations in shearing flows of liquid-crystalline polymers, *Macromolecules* 24 (1991) 6270-6282.
- [22] L. Onsager, The effects of shape on the interaction of colloidal particles", *Ann. (N. Y.) Acad. Sci.* 51 (1949) 627-659.
- [23] W. Maier and A. Saupe, Eine einfache molekulare Theorie des nematischen kristallinflüssigen Zustandes, *Z. Naturforsch.* 13A (1958) 564-566.
- [24] W. Maier and A. Saupe, Eine einfache molekular-statistische Theorie der nematischen kristallinflüssigen Phase. Teil I, *Z. Naturforsch.* 14A (1959) 882-889.
- [25] J. P. Straley, The gas of long rods as a model for lyotropic liquid crystals, *Mol. Cryst. Liq. Cryst.* 22 (1973) 333-357.
- [26] S. Hess, W. Köhler, *Formeln zur Tensor-Rechnung*, Palm & Enke, Erlangen, 1980.
- [27] R. G. Larson, *Constitutive Equations for Polymer Melts and Solutions*, Butterworth Publishers, Boston, 1988.
- [28] J. Feng, C. V. Chaubal and L. G. Leal, Closure approximations for the Doi theory: Which one to use in simulating complex flow of liquid-crystalline polymers. *J. Rheol.* 42 (1998) 1095-1119.
- [29] C. V. Chaubal and L. G. Leal and G. H. Fredrickson A Comparison of Closure Approximations for the Doi Theory of LCPs, *J. Rheol.* 39 (1995) 73-103.
- [30] C. V. Chaubal and L. G. Leal, A closure approximation for liquid-crystalline polymer models based on parametric density estimation, *J. Rheol.* 42 (1998) 177-201.
- [31] Q. Wang, Comparative studies of closure approximations in flows of liquid crystal polymers. 1. Elongational flows, *J. Non-Newton. Fluid Mech.* 72 (1997) 141-162.
- [32] Q. Wang, Comparative studies of closure approximations in flows of liquid crystal polymers. 2. Fiber flows, *J. Non-Newton. Fluid Mech.* 72 (1997) 163-185.
- [33] M. Gurr, On the use of spherical tensors and the maximum entropy method to obtain closure for anisotropic fluids, *J. Rheol.* 42 (1998) 1269-1271.
- [34] M. Grosso, P. L. Maffettone, F. Dupret, A closure approximation for nematic liquid crystals based on the canonical distribution subspace theory, *Rheol. Acta* 39 (2000) 301-310.
- [35] J. E. Hurtado, A. B. Barbat, Fourier-based maximum entropy method in stochastic dynamics, *Structural Safety* 20 (1998) 221-235.
- [36] R. G. Larson, Arrested tumbling in shearing flows of liquid-crystal polymers, *Macromolecules* 23 (1990) 3983-3992.
- [37] A. M. Jamieson, D. Gu, F. L. Chen, S. Smith, Viscoelastic behavior of nematic monodomains containing liquid crystal polymers, *Prog. Polym. Sci.* 21 (1996) 981-1033.
- [38] N. Yao, A. M. Jamieson, Transient shear flow behavior of dilute solutions of side-chain liquid-crystalline polysiloxanes in 4,4'-(n-pentyloxy)cyanobiphenyl, *Macromolecules* 31 (1998) 5399-5406.
- [39] J. L. Ericksen, *Arch. Rat. Mech. Anal.* 4 (1960) 231.

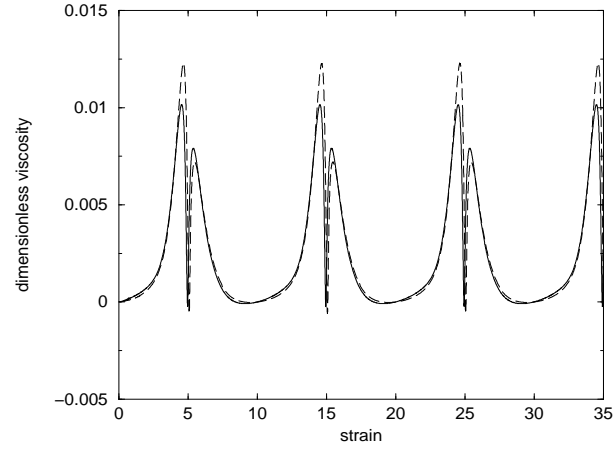


FIG. 1: Time evolution of the dimensionless shear viscosity as a function of shear strain. The nematic potential was chosen to be  $\nu_2 = 6.5$ . Solid and dashed line correspond to the dimensionless shear rate  $Pe = 5$  and  $Pe = 10$ , respectively.

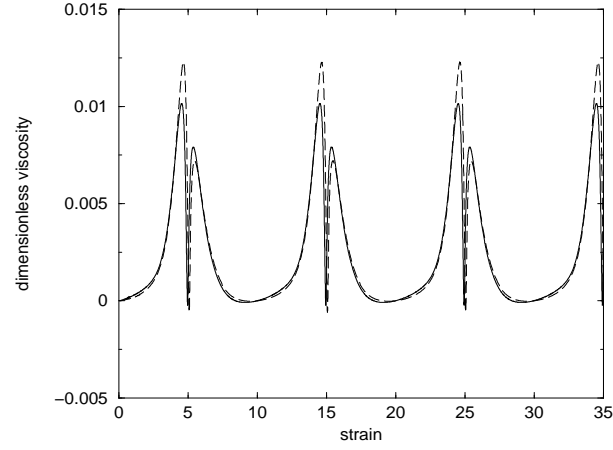


FIG. 2: Time evolution of the shear viscosity of n-octylcyanobiphenyl as a function of shear strain for shear rate  $\dot{\gamma} = 16 \text{ s}^{-1}$ . Data are taken from [37].

